

# Variability in the Structures of [4-(Aminomethyl)pyridine]silver(I) Complexes through Effects of Ligand Ratio, Anion, Hydrogen Bonding, and $\pi$ -Stacking

Rodney P. Feazell, Cody E. Carson, and Kevin K. Klausmeyer\*

Department of Chemistry and Biochemistry, Baylor University, Waco, Texas 76798

Received September 27, 2005

The reaction of the asymmetric 4-(aminomethyl)pyridine (4-amp) ligand with silver(I) salts of trifluoromethanesulfonate (triflate, OTf<sup>-</sup>), trifluoroacetate (tfa<sup>-</sup>), or tetrafluoroborate (BF<sub>4</sub><sup>-</sup>) have produced a variety of one- and two-dimensional structural motifs depending upon the ratio in which the components are mixed. When the proportion of ligand to metal is 1:1, linear coordination polymers are formed with silver(I) OTf<sup>-</sup> (**1**) and tfa<sup>-</sup> (**2**). Altering the ratio to 2:1, a linear polymer of corner-shared boxes (**3**) is formed with tfa<sup>-</sup>, a linear box-in-box “chain link” polymer (**4**) is formed with OTf<sup>-</sup>, and a two-dimensional sheet (**5**) is constructed with BF<sub>4</sub><sup>-</sup>. Addition of 5,5′-dimethyl-2,2′-bipyridine to a solution of 4-ampAgBF<sub>4</sub> disrupts the polymerization of the previous structure and results in the construction of the infinite metal–metal bound strings of **6a** regardless of ratio of amp to silver present. H-bonding,  $\pi$ -stacking, and closed-shell Ag–Ag interactions are all involved in the overall conformations of the final structures.

## Introduction

Recent interest in the rational design and construction of novel discrete and polymeric metal–organic coordination complexes has reached a new high due to the realization of their potential for use as functional materials.<sup>1–16</sup> Designed

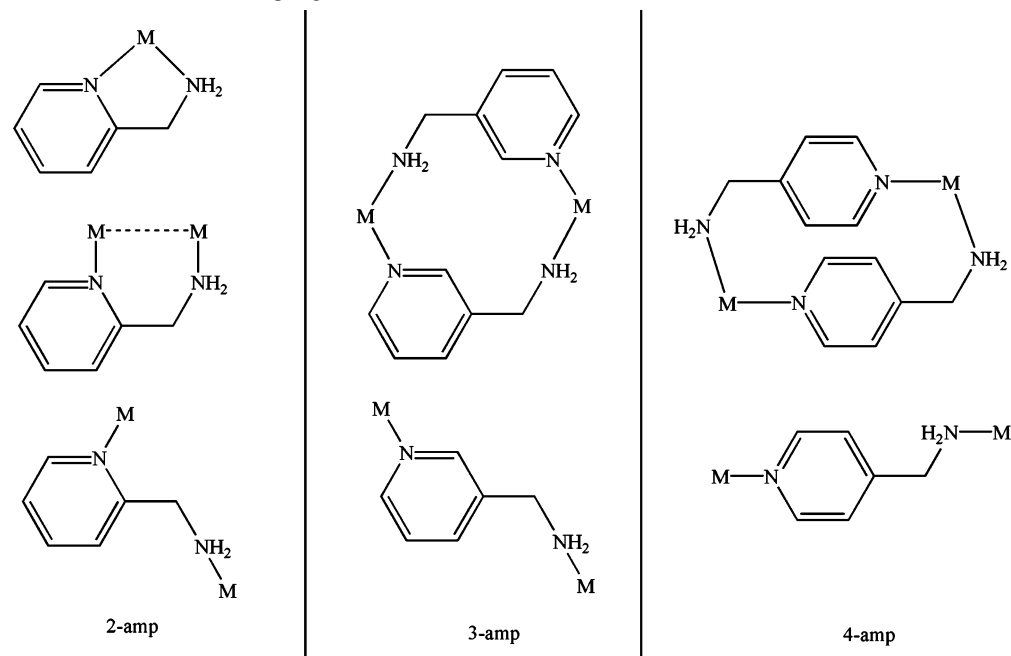
coordination architectures have found application in fields as far spread as catalysis, molecular recognition, sieving, separation, and nonlinear optics.<sup>3,15,17–23</sup> Supramolecular chemists have typically fine-tuned the properties of these complexes by using modifications in functionality, rigidity, or geometry of the basis ligand or by changes in solvent or counterion in charged systems.<sup>20,23–41</sup> Others still have made

\* To whom correspondence should be addressed. Fax: (254) 710-4272. E-mail: Kevin\_Klausmeyer@baylor.edu.

- (1) Cui, G.-H.; Li, J.-R.; Tian, J.-L.; Bu, X.-H.; Batten, S. R. *Cryst. Growth Des.* **2005**, *5*, 1775–1780.
- (2) Cui, Y.; Ngo, H. L.; White, P. S.; Lin, W. *Inorg. Chem.* **2003**, *42*, 652–654.
- (3) Evans, O. R.; Lin, W. *Acc. Chem. Res.* **2002**, *35*, 511–522.
- (4) Wei, Y.; Hou, H.; Li, L.; Fan, Y.; Zhu, Y. *Cryst. Growth Des.* **2005**, *5*, 1405–1413.
- (5) Xie, Y.-B.; Li, J.-R.; Zhang, C.; Bu, X.-H. *Cryst. Growth Des.* **2005**, *5*, 1743–1749.
- (6) Seidel, S. R.; Stang, P. J. *Acc. Chem. Res.* **2002**, *35*, 972–983.
- (7) Moulton, B.; Zaworotko, M. J. *Chem. Rev.* **2001**, *101*, 1629–1658.
- (8) Batten, S. R.; Hoskins, B. F.; Moubaraki, B.; Murray, K. S.; Robson, R. *J. Chem. Soc., Dalton Trans.* **1999**, 2977–2986.
- (9) Eddaoudi, M.; Li, H.; Yaghi, O. M. *J. Am. Chem. Soc.* **2000**, *122*, 1391–1397.
- (10) Long, D.-L.; Blake, A. J.; Champness, N. R.; Wilson, C.; Schröder, M. *J. Am. Chem. Soc.* **2001**, *123*, 3401–3402.
- (11) Masaoka, S.; Furukawa, S.; Chang, H.-C.; Mizutani, T.; Kitagawa, S. *Angew. Chem., Int. Ed.* **2001**, *40*, 3817–3819.
- (12) Hagrman, P. J.; Hagrman, D.; Zubieta, J. *Angew. Chem., Int. Ed.* **1999**, *38*, 2638–2684.
- (13) Batten, S. R.; Robson, R. *Angew. Chem., Int. Ed.* **1998**, *37*, 1460–1494.
- (14) Wu, C.-D.; Lu, C.-Z.; Yang, W.-B.; Zhuang, H.-H.; Huang, J.-S. *Inorg. Chem.* **2002**, *41*, 3302–3307.
- (15) Blake, A. J.; Champness, N. R.; Hubberstey, P.; Li, W.-S.; Withersby, M. A.; Schroder, M. *Coord. Chem. Rev.* **1999**, *183*, 117–138.

- (16) Mukherjee, P. S.; Konar, S.; Zangrando, E.; Mallah, T.; Ribas, J.; Chaudhuri, N. R. *Inorg. Chem.* **2003**, *42*, 2695–2703.
- (17) Fujita, M.; Kwon, Y. J.; Washizu, S.; Ogura, K. *J. Am. Chem. Soc.* **1994**, *116*, 1151–1152.
- (18) Kasai, K.; Aoyagi, M.; Fujita, M. *J. Am. Chem. Soc.* **2000**, *122*, 2140–2141.
- (19) Kitagawa, S.; Kitaura, R.; Noro, S.-i. *Angew. Chem., Int. Ed.* **2004**, *43*, 2334–2375.
- (20) Zheng, S.-L.; Tong, M.-L.; Chen, X.-M. *Coord. Chem. Rev.* **2003**, *246*, 185–202.
- (21) Erxleben, A. *Coord. Chem. Rev.* **2003**, *246*, 203–228.
- (22) Lu, J. Y. *Coord. Chem. Rev.* **2003**, *246*, 327–347.
- (23) Khlobystov, A. N.; Blake, A. J.; Champness, N. R.; Lemenovskii, D. A.; Majouga, A. G.; Zyk, N. V.; Schröder, M. *Coord. Chem. Rev.* **2001**, *222*, 155–192.
- (24) Park, K.-M.; Yoon, I.; Seo, J.; Lee, J.-E.; Kim, J.; Choi, K. S.; Jung, O.-S.; Lee, S. S. *Cryst. Growth Des.* **2005**, *5*, 1707–1709.
- (25) Lu, J. Y.; Cabrera, B. R.; Wang, R.-J.; Li, J. *Inorg. Chem.* **1999**, *38*, 4608–4611.
- (26) Janiak, C. *J. Chem. Soc., Dalton Trans.* **2003**, 2781–2804.
- (27) Xie, Y.-B.; Li, J.-R.; Bu, X.-H. *Polyhedron* **2005**, *24*, 413–418.
- (28) Sampanthar, J. T.; Vittal, J. J. *Cryst. Eng.* **2000**, *3*, 117–133.
- (29) Feazell, R. P.; Carson, C. E.; Klausmeyer, K. K. *Acta Crystallogr., Sect. C* **2004**, *C60*, m598–m600.
- (30) Feazell, R. P.; Carson, C. E.; Klausmeyer, K. K. *Inorg. Chem.* **2005**, *44*, 996–1005.

Scheme 1. Typical Coordination Modes of amp Ligands with Silver(I) Salts



notable contributions to the field utilizing the noncovalent  $\pi$ -stacking or H-bonding interactions to impart desired characteristics on coordination complexes.<sup>13,42–46</sup> Though a wealth of information is available on crystal engineering studies employing the aforementioned methods, the equally effectual practice of stoichiometric control has gone largely unexplored and thus unexploited.<sup>25,47</sup> Only recently have we and a handful of other researchers taken interest in investigating the effect that ratio dependence can impart upon conformation, dimensionality, and physical properties of supramolecular species.<sup>29,31–33,48–50</sup> In several of these recent

studies we have demonstrated that drastic structural modifications can be forced upon coordination complexes through variations in the ratio of ligand to metal, particularly in those metals that have the capacity to readily accept changes in their coordination number and geometry.<sup>29,31–33</sup>

Herein we continue our comprehensive study of the structural effects brought on by changes in ratio of the series of isomeric aminomethylpyridine (amp) ligands shown in Scheme 1 with various silver(I) salts. With the factors affecting the structural characteristics of the 2- and 3-amp-AgX (X = BF<sub>4</sub><sup>-</sup>, tfa<sup>-</sup>, or OTf<sup>-</sup>) complexes being previously discussed,<sup>29,31–33</sup> we now report on the ratio dependence of 4-ampAgX, with the present account also illustrating the relationship between anion and stoichiometric effects. It is seen that the degree of interaction that the anions (particularly those of oxygen) have with the metal centers as well as the extent of the H-bonding network present is related to the ratio of ligand to metal present in the structure. Also affecting the overall growth of the complexes is the  $\pi$ -stacking interactions that occur between adjacent pyridyl rings.

## Experimental Section

**General Procedures.** All experiments were carried out under an argon atmosphere, using a Schlenk line and standard Schlenk techniques. Glassware was dried at 120 °C for several hours prior to use. All reagents were stored in an inert atmosphere glovebox; solvents were distilled under nitrogen from the appropriate drying agent immediately before use. 4-Aminomethylpyridine, 5,5'-dimethyl-2,2'-bipyridine, and 2,2'-bipyridine were purchased from Aldrich and used as received. Silver(I) tetrafluoroborate (BF<sub>4</sub>), silver(I) trifluoroacetate (tfa), and silver(I) trifluoromethanesulfonate (OTf) were purchased from Strem Chemicals Inc. and used as received. <sup>1</sup>H NMR spectra were recorded at 360.13 MHz on a

- (31) Feazell, R. P.; Carson, C. E.; Klausmeyer, K. K. *Eur. J. Inorg. Chem.* **2005**, 3287–3297.  
 (32) Feazell, R. P.; Carson, C. E.; Klausmeyer, K. K. Submitted for publication in *Inorg. Chem.* **2005**.  
 (33) Feazell, R. P.; Carson, C. E.; Klausmeyer, K. K. Submitted for publication in *Inorg. Chem.* **2005**.  
 (34) Goher, M. A. S.; Hafez, A. K.; Abu-Youssef, M. A. M.; Badr, A. M. A.; Gspan, C.; Mautner, F. A. *Polyhedron* **2004**, *23*, 2349–2356.  
 (35) Dong, Y.-B.; Zhao, X.; Huang, R.-Q.; Smith, M. D.; Loye, H.-C. *Inorg. Chem.* **2004**, *43*, 5603–5612.  
 (36) Eisler, D. J.; Puddephatt, R. J. *Cryst. Growth Des.* **2005**, *5*, 57–59.  
 (37) Pickering, A. L.; Long, D.-L.; Cronin, L. *Inorg. Chem.* **2004**, *43*, 4953–4961.  
 (38) Vetrichelvan, M.; Lai, Y.-H.; Mok, K. F. *Eur. J. Inorg. Chem.* **2004**, *2004*, 2086–2095.  
 (39) Zaman, M. B.; Udachin, K.; Ripmeester, J. A.; Smith, M. D.; zur Loye, H.-C. *Inorg. Chem.* **2005**, *44*, 5047–5059.  
 (40) Klausmeyer, K. K.; Feazell, R. P.; Reibenspies, J. H. *Inorg. Chem.* **2004**, *43*, 1130–1136.  
 (41) Seward, C.; Chan, J.; Song, D.; Wang, S. *Inorg. Chem.* **2003**, *42*, 1112–1120.  
 (42) Yaghi, O. M.; Li, H.; Davis, C.; Richardson, D.; Groy, T. L. *Acc. Chem. Res.* **1998**, *31*, 474–484.  
 (43) Zaworotko, M. J. *Angew. Chem., Int. Ed.* **2000**, *39*, 3052–3054.  
 (44) Philp, D.; Stoddart, J. F. *Angew. Chem., Int. Ed. Engl.* **1996**, *35*, 1154–1196.  
 (45) Manners, I. *Angew. Chem., Int. Ed. Engl.* **1996**, *35*, 1602–1621.  
 (46) Feazell, R. P.; Carson, C. E.; Klausmeyer, K. K. *Acta Crystallogr., Sect. E* **2005**, m1694–m1696.  
 (47) Cotton, F. A.; Lin, C.; Murillo, C. A. *J. Chem. Soc., Dalton Trans.* **2001**, 499–501.  
 (48) Oh, M.; Stern, C. L.; Mirkin, C. A. *Inorg. Chem.* **2005**, *44*, 2647–2653.

- (49) Dong, Y.-B.; Wang, H.-Y.; Ma, J.-P.; Shen, D.-Z.; Huang, R.-Q. *Inorg. Chem.* **2005**, *44*, 4679–4692.  
 (50) Sailaja, S.; Rajasekharan, M. V. *Inorg. Chem.* **2003**, *42*, 5675–5684.

Bruker Spectrospin 360 MHz spectrometer. Elemental analyses were performed by Atlantic Microlabs Inc., Norcross, GA.

**General Synthesis.** General procedures for the synthesis of compounds **1–6a** involve the addition of a 5 mL acetonitrile solution of 4-aminomethylpyridine to a stirred solution of the appropriate silver salt in 5 mL of acetonitrile. The mixtures are then allowed to stir for 10 min and then dried in vacuo to leave white or off-white powders. All flasks are shielded from light with aluminum foil to prevent the photodecomposition of the silver compounds. Crystals of compounds **2–5** were grown by layering ether over acetonitrile solutions at 5 °C. Crystals of compound **1** and **6a** were grown by vapor diffusion of ether into acetonitrile solutions at 5 °C. The amounts of reagents used, yields, and analytical data are presented below as well as any modifications to the general synthetic procedure. Percent yields are based upon the amount of silver salt used.

**Synthesis of Ag(4-amp)OTf (1).** This reaction used 4-aminomethylpyridine (0.100 g, 0.924 mmol) added to AgOTf (0.237 g, 0.922 mmol) to leave a white powder in 96% yield (0.323 g, 0.89 mmol) upon evaporation of the solvent. Colorless plates of **1** were formed. <sup>1</sup>H NMR (CD<sub>3</sub>CN, 298 K) δ: 3.81 s, br, 2H, (–NH<sub>2</sub>–); 3.97 s, 2H, (–CH<sub>2</sub>–); 7.46 m, 2H; 8.43 m, 2H. Anal. Calcd for AgC<sub>7</sub>H<sub>8</sub>N<sub>2</sub>O<sub>3</sub>SF<sub>3</sub>: C, 25.80; H, 2.47; N, 8.56. Found: C, 26.27; H, 2.33; N, 8.77.

**Synthesis of Ag(4-amp)tfa (2).** This reaction used 4-aminomethylpyridine (0.100 g, 0.924 mmol) and Agtfa (0.204 g, 0.925 mmol). Solvent was removed in vacuo, and the resulting white powder was isolated in 97% yield (0.295 g, 0.897 mmol). Colorless blocks were formed. <sup>1</sup>H NMR (CD<sub>3</sub>CN, 298 K) δ: 3.81 s, br, 2H, (–NH<sub>2</sub>–); 3.97 s, 2H, (–CH<sub>2</sub>–); 7.54 m, 2H; 8.43 m, 2H. Anal. Calcd for AgC<sub>8</sub>H<sub>8</sub>N<sub>2</sub>O<sub>2</sub>F<sub>3</sub>: C, 29.20; H, 2.45; N, 8.51. Found: C, 29.38; H, 2.39; N, 8.40.

**Synthesis of Ag(4-amp)<sub>2</sub>tfa (3).** The reaction was done in a 2:1 ratio of 4-aminomethylpyridine (0.100 g, 0.924 mmol) to Agtfa (0.102 g, 0.462 mmol). A white precipitate was observed upon addition of the 4-aminomethylpyridine. After the solvent was removed in vacuo, a white powder was obtained in 94% yield (0.190 g, 0.432 mmol). Colorless blocks were formed by layering ether over an acetonitrile suspension of **3** at 5 °C. <sup>1</sup>H NMR (CD<sub>3</sub>OD, 298 K) δ: 4.57 s, br, 2H, (–NH<sub>2</sub>–); 5.46 s, 2H, (–CH<sub>2</sub>–); 8.11 m, 2H; 9.07 2H. Anal. Calcd for AgC<sub>14</sub>H<sub>16</sub>N<sub>4</sub>O<sub>2</sub>F<sub>3</sub>: C, 38.46; H, 3.69; N, 12.82. Found: C, 38.24; H, 3.57; N, 12.54.

**Synthesis of Ag(4-amp)<sub>2</sub>(OTf) (4).** This reaction used 2 equiv of 4-aminomethylpyridine (0.100 g, 0.924 mmol) added to AgOTf (0.118 g, 0.462 mmol). A clear, colorless oil was left upon evaporation of the solvent. The oil was dissolved in a small amount of CH<sub>3</sub>CN and then precipitated with ether resulting in a white fluffy powder in 78% yield (0.171 g, 0.180 mmol). Colorless blocks were formed. <sup>1</sup>H NMR (CD<sub>3</sub>CN, 298 K) δ: 3.26 s, br, 4H, (–NH<sub>2</sub>–); 3.91 s, 2d, (–CH<sub>2</sub>–); 7.36 m, 4H; 8.46 m, 4H. Anal. Calcd for AgC<sub>13</sub>H<sub>16</sub>N<sub>4</sub>O<sub>3</sub>SF<sub>3</sub>: C, 33.00; H, 3.41; N, 11.84. Found: C, 33.18; H, 3.24; N, 11.75.

**Synthesis of Ag(4-amp)<sub>2</sub>BF<sub>4</sub> (5).** This reaction used 2 equiv of 4-aminomethylpyridine (0.100 g, 0.924 mmol) added to AgBF<sub>4</sub> (0.090 g, 0.462 mmol). Upon evaporation of the solvent an off-white powder was isolated in 84% yield (0.160 g, 0.389 mmol). Colorless plates were formed. <sup>1</sup>H NMR (CD<sub>3</sub>CN, 298 K) δ: 2.79 s, br, 4H, (–NH<sub>2</sub>–); 3.89 s, 4H, (–CH<sub>2</sub>–); 7.36 m, 2H; 8.38 m, 2H. Anal. Calcd for AgC<sub>12</sub>H<sub>16</sub>N<sub>4</sub>BF<sub>4</sub>: C, 35.07; H, 3.92; N, 13.63. Found: C, 35.03; H, 3.78; N, 13.33.

**Synthesis of Ag<sub>2</sub>(2,2'-bipy)<sub>2</sub>-μ-(4-amp)(BF<sub>4</sub>)<sub>2</sub> (6).** To a stirred solution of 1 equiv of 4-aminomethylpyridine (0.100 g, 0.93 mmol) in 5 mL of CH<sub>3</sub>CN was added 2 equiv of AgBF<sub>4</sub> (0.360 g, 1.82

mmol) in 5 mL more CH<sub>3</sub>CN. This was allowed to stir for 5 min, and then a solution of 2,2'-bipyridine (0.289 g, 1.82 mmol) in 5 mL of CH<sub>3</sub>CN was added. This mixture was allowed to stir for an additional 10 min, and then the solvent was removed in vacuo to leave a light yellow powder in 84% yield (0.631 g, 0.78 mmol). <sup>1</sup>H NMR (CD<sub>3</sub>CN, 298 K) δ: 2.17 s, br, 2H, (–NH<sub>2</sub>–); 3.98 s, 2H, (–CH<sub>2</sub>–); 8.69 m, 8H; 8.44 m, 9H; 8.08 m, 2H; 7.59 m, 1H. Anal. Calcd for Ag<sub>2</sub>C<sub>29</sub>H<sub>28</sub>N<sub>7</sub>B<sub>2</sub>F<sub>8</sub>: C, 40.32; H, 3.27; N, 11.35. Found: C, 40.68; H, 3.26; N, 11.20.

**Synthesis of Ag<sub>2</sub>(5,5'-bismethyl-2,2'-bpy)<sub>2</sub>(4-amp)(BF<sub>4</sub>)<sub>2</sub>(6a).** The procedure for this reaction is the same as that used for the preparation of **6** and used 1 equiv of 4-aminomethylpyridine (0.150 g, 1.39 mmol) added to 2 equiv of AgBF<sub>4</sub> (0.540 g, 2.77 mmol). After stirring for 5 min, 2 equiv of 5,5'-dimethyl-2,2'-bipyridine was added (0.510 g, 2.77 mmol). After an additional 10 min of stirring the solvent was removed in vacuo to leave a white powder in 89% yield (1.07 g, 1.23 mmol). <sup>1</sup>H NMR (CD<sub>3</sub>CN, 298K) δ: 2.39 s, 12H (Me); 2.57 2s, br, 2H (–NH<sub>2</sub>–); 3.87 s, 2H (–CH<sub>2</sub>–); 7.33 m, 4H; 7.81 dd, 2H; 8.05 dd, 2H; 8.42 m, 6H.

**X-ray Crystallographic Analysis.** Crystallographic data were collected on crystals with dimensions 0.171 × 0.109 × 0.047 mm for **1**, 0.110 × 0.100 × 0.070 mm for **2**, 0.090 × 0.060 × 0.060 mm for **3**, 0.249 × 0.230 × 0.153 mm for **4**, 0.152 × 0.114 × 0.112 mm for **5**, and 0.264 × 0.220 × 0.189 mm for **6a**. Data were collected at 110 K on a Bruker X8 Apex using Mo Kα radiation (λ = 0.710 73 Å). The structures were solved by direct methods and refined by full-matrix least-squares refinement on *F*<sup>2</sup>. Multiscan absorption corrections were applied using the program SADABS.<sup>51</sup> Crystal data are presented in Table 1, and selected interatomic distances, angles, and other important distances are given in Tables 2 and 3. All of the data were processed using the Bruker AXS SHELXTL software, version 6.10.<sup>52</sup> Unless otherwise noted, all non-hydrogen atoms were refined anisotropically and hydrogen atoms were placed in calculated positions. The positions of the amine hydrogens were allowed to refine. The structure of **1** contains two solvent acetonitrile molecules in the lattice. The trifluoroacetate anion of compound **3** is disordered over two positions across a mirror plane. The structure of compound **6a** contains two solvent acetonitrile molecules and a BF<sub>4</sub><sup>–</sup> anion which is disordered over three positions. The smaller two occupancies of the disorder are refined as isotropic spheres.

## Results and Discussion

**Synthesis.** The 4-aminomethylpyridine complexes **1–5** were synthesized by the direct reaction of the 4-amp ligand with the appropriate silver(I) salt (OTf<sup>–</sup>, tfa<sup>–</sup>, or BF<sub>4</sub><sup>–</sup>) in varying ratios. All of the compounds containing only 4-amp and silver were isolated as fine white to off-white powders. The 2:1 complex, **3**, is the only compound reported herein that shows only sparing solubility in acetonitrile and precipitates in the correct ratio upon formation. As a result, crystallization of **3** was achieved with some difficulty from saturated CH<sub>3</sub>CN solutions grown over several weeks and the <sup>1</sup>H NMR spectrum is reported in CD<sub>3</sub>OD solvent. Compounds **6** and **6a** were isolated as fine yellow and off-white powders, respectively. Both were formed by the addition of the corresponding bipyridyl ligand to solutions

(51) Sheldrick, G. M. *SADABS*; University of Goettingen: Goettingen, Germany, 1997.

(52) Sheldrick, G. M. *SHELXTL*, version 6.10; Bruker AXS, Inc.: Madison, WI, 2000.

**Table 1.** Crystallographic Data for Compounds **1–6a**

	<b>1</b>	<b>2</b>	<b>3</b>	<b>4</b>	<b>5</b>	<b>6a</b>
formula	C <sub>11</sub> H <sub>14</sub> AgF <sub>3</sub> N <sub>4</sub> O <sub>3</sub> S	C <sub>16</sub> H <sub>16</sub> Ag <sub>2</sub> F <sub>6</sub> N <sub>4</sub> O <sub>4</sub>	C <sub>14</sub> H <sub>16</sub> AgF <sub>3</sub> N <sub>4</sub> O <sub>2</sub>	C <sub>13</sub> H <sub>16</sub> AgF <sub>3</sub> N <sub>4</sub> O <sub>3</sub> S	C <sub>12</sub> H <sub>16</sub> AgBF <sub>4</sub> N <sub>4</sub>	C <sub>34</sub> H <sub>38</sub> Ag <sub>2</sub> B <sub>2</sub> F <sub>8</sub> N <sub>8</sub>
formula weight	447.19	658.07	437.18	473.23	410.97	948.08
<i>a</i> (Å)	6.6871(7)	9.3793(7)	12.4623(14)	7.9279(4)	10.2034(3)	18.76(1)
<i>b</i> (Å)	25.806(2)	10.5770(7)	18.273(2)	10.0058(4)	13.3334(4)	30.12(1)
<i>c</i> (Å)	9.3785(8)	11.6814(8)	7.4106(8)	11.5612(5)	12.3596(4)	6.690(3)
α (deg)		95.210(2)		98.964(2)		
β (deg)	92.135(3)	91.393(2)	92.986(4)	108.141(2)	103.690(2)	91.96(1)
γ (deg)		114.234(2)		95.402(2)		
Z	4	2	4	2	4	4
space group	<i>P</i> 2 <sub>1</sub> / <i>c</i>	<i>P</i> $\bar{1}$	<i>C</i> 2/ <i>m</i>	<i>P</i> $\bar{1}$	<i>P</i> 2 <sub>1</sub> / <i>c</i>	<i>P</i> 2 <sub>1</sub> / <i>c</i>
<i>D</i> <sub>calcd</sub> (g cm <sup>-3</sup> )	1.837	2.082	1.723	1.847	1.671	1.666
μ (mm <sup>-1</sup> )	1.424	1.949	1.241	1.359	1.273	1.113
2θ <sub>max</sub> (deg)	32.15	26.35	25.30	25.00	28.27	25.00
reflns measured	26679	15985	7120	29250	21977	29173
reflns used ( <i>R</i> <sub>int</sub> )	4711 (0.0318)	4258 (0.0325)	1572 (0.0301)	4113 (0.0344)	3961 (0.0299)	7788 (0.0446)
restraints/params	0/216	0/289	0/133	0/226	0/199	31/528
<i>R</i> <sub>1</sub> <sup>a</sup> [ <i>I</i> > 2σ( <i>I</i> )]	0.0344	0.0248	0.0288	0.0187	0.0255	0.0394
w <i>R</i> <sub>2</sub> <sup>b</sup> [ <i>I</i> > 2σ( <i>I</i> )]	0.0538	0.0585	0.0624	0.0473	0.0624	0.1039
<i>R</i> ( <i>F</i> <sub>o</sub> <sup>2</sup> ), (all data)	0.0493	0.0328	0.0408	0.0199	0.0364	0.0448
<i>R</i> <sub>w</sub> ( <i>F</i> <sub>o</sub> <sup>2</sup> ), (all data)	0.0578	0.0609	0.0674	0.0477	0.0698	0.1072
GOF on <i>F</i> <sup>2</sup>	1.075	1.073	1.012	1.052	1.042	1.078

<sup>a</sup> *R*<sub>1</sub> = [Σw(*F*<sub>o</sub> - *F*<sub>c</sub>)<sup>2</sup>/Σw*F*<sub>o</sub><sup>2</sup>]<sup>1/2</sup>. <sup>b</sup> w*R*<sub>2</sub> = [Σ[w(*F*<sub>o</sub><sup>2</sup> - *F*<sub>c</sub><sup>2</sup>)/Σw(*F*<sub>o</sub><sup>2</sup>)<sup>1/2</sup>]<sup>2</sup>; w = 1/[c(*F*<sub>o</sub><sup>2</sup>) + (*aP*)<sup>2</sup> + *bP*], where *P* = [max(*F*<sub>o</sub><sup>2</sup>, 0) + 2(*F*<sub>c</sub><sup>2</sup>)]/3.

**Table 2.** Selected Bond Lengths (Å), Angles (deg), and Important Distances for **1** and **2**<sup>a</sup>

		<b>1</b>			
Ag1–N1		2.158(2)	Ag1–N2#1	2.164(2)	
N1–Ag1–N2#1		172.73(7)	C2–C3–C6–N2	5.2(3)	
		D–H	H···A	D···A	∠(DHA)
N2–H1···O1#1		0.86(3)	2.29(3)	3.134(3)	166(2)
N2–H2···O3#2		0.85(3)	2.18(3)	2.986(3)	159(2)
		<b>2</b>			
Ag1–N2#1		2.143(2)	Ag1–N1	2.146(2)	
Ag2–N3		2.157(2)	Ag2–N4#2	2.173(2)	
Ag2–O1		2.565(2)	N2#1–Ag1–N1	170.68(9)	
N3–Ag2–N4#2		169.99(9)	N3–Ag2–O1	103.51(8)	
N4#2–Ag2–O1		81.52(8)	C2–C3–C6–N2	7.4(4)	
C8–C9–C12–N4		23.1(4)			
		D–H	H···A	D···A	∠(DHA)
N2–H2A···O3#1		0.80(3)	2.16(3)	2.863(3)	148(3)
N2–H2B···O2#2		0.93(3)	1.93(3)	2.833(3)	162(3)
N4–H4A···O4#3		0.82(3)	2.17(3)	2.974(3)	166(3)
N4–H4B···O4#4		0.90(3)	2.10(3)	2.980(3)	168(3)

<sup>a</sup> Symmetry transformations used to generate equivalent atoms. For **1**: #1 = *x*, *y*, *z* - 1; #2 = -*x* + 1, -*y* + 1, -*z* + 2; #3 = -*x*, -*y* + 1, -*z* + 2. For **2**: #1 = *x* + 1, *y*, *z*; #2 = *x* - 1, *y*, *z*; #3 = -*x*, -*y* + 1, -*z* + 1; #4 = -*x*, -*y* + 2, -*z* + 1; #5 = *x*, *y*, *z* - 1; #6 = -*x* + 1, -*y* + 1, -*z* + 1.

of 4-amp and AgBF<sub>4</sub><sup>-</sup>. The formation of **6** and **6a** was seen to be independent of the ratio of 4-amp to Ag<sup>+</sup>, so long as there was sufficient 4-amp present to bridge each pair of bipy-capped silver ions. 4-amp in excess of 1/2 equiv was always isolated in the crude product as uncoordinated ligand.

**X-ray Crystal Structures.** The range of metal coordination environments in the crystal structures of compounds **1–6a** is demonstrative of the facility with which the silver-(I) cation varies its coordination sphere to accept the number and type of donors required of it. Coordination numbers from 2 to 5 are seen encompassing geometries of linear (**1**, **2**), T-shaped (**2**), trigonal planar (**6a**), tetrahedral (**3–5**), and trigonal bipyramidal (**6a**). The conformation of the ligands is seen to be quite sensitive to counterion effects due to the strong H-bonding propensity of the amine donor when oxygen-containing anions are present. However, the silver environment is just as susceptible, if not more so, to change

when added equivalents of ligand are presented to it. Compounds **1** and **2** both display a 1:1 ratio of 4-amp ligand to metal with variances between the two arising from the difference in basicity of triflate versus trifluoroacetate. The less strongly interacting tetrafluoroborate 1:1 complex with 4-amp has previously been reported and displays a structural motif similar to those of the first two compounds reported herein.<sup>50</sup> A second equivalent of 4-amp effectively forces the metal center to accept a tetrahedral geometry to receive the two added N-donors present. As a result, compounds **3–5** all adopt similar 4-coordinate metal environments of two each amine and pyridyl donors. However, the supramolecular structures of these compounds are again quite varied due to the differences in interactions of the anions with the amine protons. Interestingly, the intermediate 3:2 ratio of ligand to metal that we were able to achieve with both 2-amp and 3-amp has been thus far elusive to isolate. This is likely due



**Table 3.** Selected Bond Lengths (Å), Angles (deg), and Important Distances for **3**, **4**, **5**, and **6a**<sup>a</sup>

<b>3</b>				
Ag1–N2#1	2.321(3)	Ag1–N2#2	2.321(3)	
Ag1–N1#3	2.324(3)	Ag1–N1	2.324(3)	
N2#1–Ag1–N2#2	100.2(2)	N2#1–Ag1–N1#3	101.3(1)	
N2#2–Ag1–N1#3	121.26(9)	N2#1–Ag1–N1	121.26(9)	
N2#2–Ag1–N1	101.3(1)	N1#3–Ag1–N1	112.1(1)	
C2–C3–C6–N2	91.6(4)	Ag1...Ag1#1	6.7848(7)	
	D–H	H...A	D...A	∠(DHA)
N2–H2B...O1#1	0.88(4)	2.15(4)	3.010(4)	166(4)
N2–H2A...O2#2	0.79(4)	2.40(4)	3.174(4)	166(4)
<b>4</b>				
Ag1–N3	2.276(1)	Ag1–N1#1	2.346(1)	
Ag1–N4#2	2.391(1)	Ag1–N2	2.431(1)	
N3–Ag1–N1#1	119.90(5)	N3–Ag1–N4#2	117.91(5)	
N1#1–Ag1–N4#2	109.55(5)	N3–Ag1–N2	118.19(5)	
N1#1–Ag1–N2	93.50(4)	N4#2–Ag1–N2	92.07(4)	
C9–C8–C7–N3	66.0(2)	C3–C2–C1–N1	39.8(2)	
Ag1...Ag1#7	6.9946(4)	N1#1...N1#7	13.577(3)	
	D–H	H...A	D...A	∠(DHA)
N1–H1C...O1#1	0.84(2)	2.21(2)	3.022(2)	165.2(2)
N1–H1D...O1#2	0.86(2)	2.40(2)	3.259(2)	178.9(2)
N3–H3A...O2#3	0.84(2)	2.25(2)	3.054(2)	160.4(2)
N3–H3B...O3#4	0.88(2)	2.19(2)	3.037(2)	162.8(2)
<b>5</b>				
Ag1–N1	2.280(2)	Ag1–N2#1	2.327(2)	
Ag1–N4#2	2.346(2)	Ag1–N3	2.380(2)	
N1–Ag1–N2#1	126.60(7)	N1–Ag1–N4#2	116.96(7)	
N2#1–Ag1–N4#2	99.86(7)	N1–Ag1–N3	105.85(6)	
N2#1–Ag1–N3	102.97(7)	N4#2–Ag1–N3	101.23(7)	
C6–C2–C1–N2	73.0(3)	C9–C8–C7–N4	92.4(3)	
Ag1...Ag1#1	6.5094(3)	Ag1...Ag1#6	20.0112(6)	
	D–H	H...A	D...A	∠(DHA)
N2–H2A...F1#1	0.87(3)	2.37(3)	3.071(3)	138(3)
N2–H2B...F4	0.83(3)	2.28(3)	3.091(2)	165(3)
N4–H4A...F4#2	0.79(3)	2.39(3)	3.158(2)	165(3)
N4–H4A...F2#3	0.79(3)	2.49(3)	3.120(3)	138(2)
N4–H4B...F1#4	0.88(3)	2.49(3)	3.283(3)	150(2)
<b>6a</b>				
Ag1–N1	2.161(3)	Ag1–N3	2.256(3)	
Ag1–N4	2.335(3)	Ag2–N2	2.138(3)	
Ag2–N5	2.240(3)	Ag2–N6	2.339(3)	
Ag2–Ag2#1	3.348(1)	Ag2–Ag2#2	3.348(1)	
N1–Ag1–N3	150.2(1)	N1–Ag1–N4	136.7(1)	
N3–Ag1–N4	72.8(1)	N2–Ag2–N5	153.9(1)	
N2–Ag2–N6	132.8(1)	N5–Ag2–N6	73.1(1)	
N2–Ag2–Ag2#1	83.21(8)	N5–Ag2–Ag2#1	104.44(7)	
N6–Ag2–Ag2#1	85.93(7)	N2–Ag2–Ag2#2	100.32(8)	
N5–Ag2–Ag2#2	74.00(7)	N6–Ag2–Ag2#2	88.93(7)	
Ag2#1–Ag2–Ag2#2	174.85(2)	C3–C2–C1–N1	7.4(6)	
	D–H	H...A	D...A	∠(DHA)
N1–H1C...F7#1	0.85(4)	2.12(5)	2.960(4)	171(4)
N1–H1D...F8#2	0.84(4)	2.17(5)	2.979(4)	161(4)

<sup>a</sup> Symmetry transformations used to generate equivalent atoms. For **3**: #1 =  $-x + 1/2, -y + 1/2, -z + 1$ ; #2 =  $x - 1/2, -y + 1/2, z$ ; #3 =  $-x, y, -z + 1$ ; #4 =  $x + 1/2, y - 1/2, z$ . For **4**: #1 =  $x - 1, y, z$ ; #2 =  $-x, -y + 1, -z + 1$ ; #3 =  $x + 1, y, z + 1$ ; #4 =  $-x + 2, -y + 2, -z + 1$ ; #5 =  $-x + 1, -y + 1, -z + 1$ ; #6 =  $x, y, z + 1$ ; #7 =  $-x, -y + 1, -z + 1$ . For **5**: #1 =  $-x + 1, -y + 1, -z + 1$ ; #2 =  $-x + 2, y - 1/2, -z + 1/2$ ; #3 =  $-x + 1, -y + 1, -z + 2$ ; #4 =  $-x + 2, -y + 1, -z + 1$ ; #5 =  $-x + 2, y + 1/2, -z + 3/2$ ; #6 =  $-x + 3, -y + 1, -z$ . For **6a**: #1 =  $x, -y + 3/2, z + 1/2$ ; #2 =  $x, -y + 3/2, z - 1/2$ ; #3 =  $-x + 1, -y + 1, -z$ ; #4 =  $-x + 1, -y + 1, -z + 1$ .

to the inordinately stable 4-ampAg “box” displayed in Scheme 1 that is formed when a 2:1 ratio is achieved. This “box” is constructed of a pair of head-to-tail coordinated 4-amp ligands bound to two symmetry equivalent silvers. In this arrangement the pyridyl  $\pi$ -systems of the opposing ligands are conveniently situated to interact with one another,

forming an exceptionally sound bimetallic cycle. This “box” is the common unit relating all three 2:1 structures. Compound **6** consistently produced poor quality crystals and therefore was modeled by its methylated relative, **6a**, to study the solid-state structure of the 4-amp bridged bis[Ag(I)2,2'-bipy] unit.

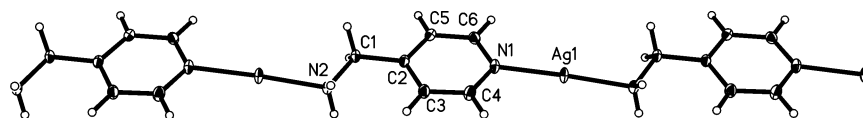


**Figure 1.** Molecular structure of the cationic polymer **1**. Ellipsoids are drawn at the 50% probability level. Solvent molecules of crystallization and anions are not shown.

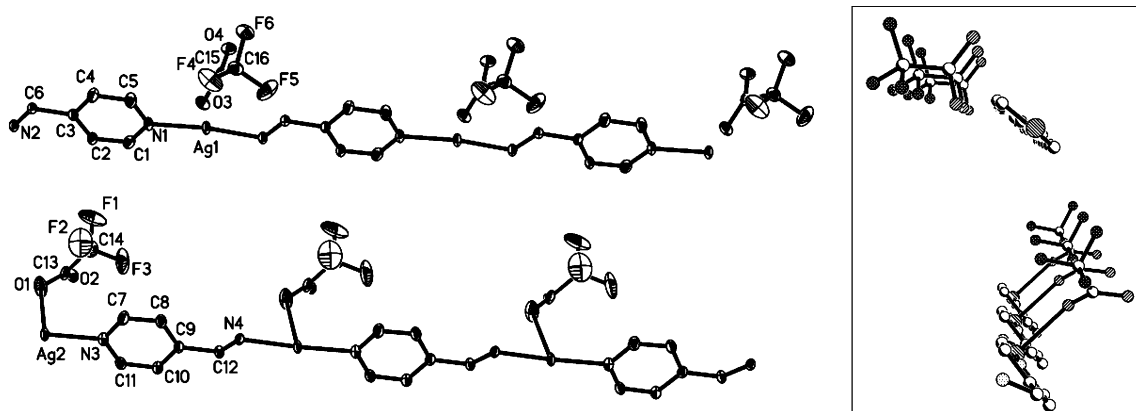


**Figure 2.** 50% thermal ellipsoid representation of the parallel polymers of **2**. Hydrogen atoms have been removed for clarity. Inset is a view down the length of the polymers showing the different approaches of the anions.

The 1:1 ratio of ligand to metal in compounds **1** and **2** causes a 2:1 ratio of N to Ag. This results in both structures adopting a preferred one-dimensional growth due to the propensity of the Ag(I) cation to be linear in a two-coordinate environment. Differences between the two structures seem to stem more from the slight differences in coordinating ability of the anions here than in the geometry about the H-bonding head of the anion as was seen in the studies of the other amp isomers.<sup>31–33</sup>

A molecular diagram showing the straight line growth of **1** is shown in Figure 1. The para substitution of the aminomethyl group on the pyridyl ring allows for a more outward conformation of the ligand in the direction of perpetuation of the structure than was achieved with the 2- or 3-amp's. What results is a polymer that is relatively thin in comparison with the bulky helical and zigzag silver(I) polymers constructed using 2- and 3-amp bridges.<sup>31–33</sup> A general planarity of the polymer is also noticed due to the orientation of the methylene–nitrogen bond nearly parallel to the plane of the pyridyl ring. This is given by the C3–C2–C1–N2 torsion angle of only 5.2(3)°. The triflate anion in this instance acts noncoordinating, preferring to hydrogen bond to the amines rather than link to the metal center, joining the polymers into a pseudo-two-dimensional sheet. Pyridyl–Ag and amine–Ag distances are similar and have typical values at 2.158(2) and 2.164(2) Å, respectively. The N–Ag–N angle is only slightly off linear at 172.73(7)°.

The 1:1 ratio of 4-amp to Agtfa produces another one-dimensional coordination polymer, **2**. In this instance, however, the structure is actually composed of two unique polymers running parallel to one another as shown in Figure 2. The polymer strands are differentiated from each other by the degree of interaction that each strand has with its associated anion. As seen in the diagram, the upper strand has a noncoordinated anion caused by the angle of approach of the tfa<sup>−</sup> to the polymer in which the CO<sub>2</sub><sup>−</sup> head of the

anion is bisected by the plane of that polymer. In the lower strand, the anion approaches from atop the pyridyl plane and is allowed within close enough proximity to bind to the metal centers with a Ag2–O1 bond length of 2.565(2) Å. As a result, both charge neutral and formally positively charged chains are used in the construction of **2**. It is also seen that the cationic polymer is more closely related to that of **1** than the anion bound polymer in terms of its planarity. In the charged polymer the –CH<sub>2</sub>–NH<sub>2</sub>– bond is again relatively close to planar with the pyridyl rings of the chain, showing an acute C2–C3–C6–N2 torsion angle of 7.4(4)°. Distortions in the opposing polymer likely caused by the coordinated tfa<sup>−</sup> result in the analogous C8–C9–C12–N4 angle being slightly larger, 23.1(4)°. The pyridyl–Ag and amine–Ag bond distances of the neutral polymer are comparable to those seen in **1** at 2.157(2) and 2.173(2) Å, respectively. The same distances in the absence of a closely associated anion are, as expected, slightly shorter at 2.146(2) and 2.143(2) Å. An interesting observation of the N–Ag–N bond angles about silvers 1 and 2 sees them nearly identical at 170.68–(9) and 169.99(9)°, respectively. This distortion is implicative of at least partial interaction between the noncoordinating tfa<sup>−</sup> and the metal center. Hydrogen bonding to O2 of the coordinated anion and to both oxygens of the noncoordinated anion serve to hold the trifluoroacetates in place as well as acting as a bridge between the parallel polymer strands.

Compounds **3–5** all display a 2:1 ratio of 4-amp to silver(I) and result from the addition of two equivalents of ligand to the appropriate silver salt. All are based around the bimetallic “box” described previously, though these smaller units are connected in different ways to construct the separate structures.

When more than a single equivalent of 4-amp is added to a solution of Agtfa, the sparingly soluble compound **3** precipitates from the solution. Recrystallization of this solid yields the structure shown in Figure 3. The unique portion

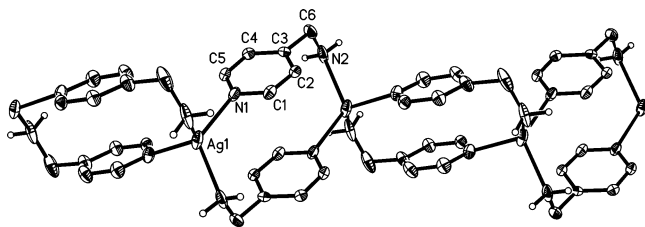


**Figure 3.** View of the cationic chain of **3**. Ellipsoids are drawn at the 30% probability level. Anions and all hydrogen atoms except for those on the amines have been removed for clarity.

of this structure is labeled in the figure and contains one ligand and one half-occupied silver(I) ion, keeping the correct ratio. When this unique part is grown through an inversion center, the biligand, bimetallic “box” that forms the basis for this and the subsequent two structures can be seen. In the construction of this box the  $-\text{CH}_2-\text{NH}_2-$  bond rotates normal to the pyridyl plane, displaying a  $\text{C}2-\text{C}3-\text{C}6-\text{N}2$  torsion angle of  $91.6(4)^\circ$  and linking two symmetry-equivalent silvers with a cross-box  $\text{Ag}-\text{Ag}$  distance of  $6.7848(7)$  Å. In this orientation the opposing pyridyl rings are situated directly adjacent to one another such that they achieve a  $\pi-\pi$  separation of approximately 3.34 Å. This favorable  $\pi$ -stacking helps account for the preference of the 4-amp  $\text{AgX}$  compounds to bypass the 3:2 ratio of ligand to metal and proceed directly to the 2:1 structures. The polymerization of **3** occurs in one dimension, forming a linear chain. The back-and-forth twisting of this chain is assisted by the H-bonding of trifluoroacetates across the face of each link. The chain itself is joined together by the sharing of the two silver occupied corners of each link with the next in line. The metal centers are in slightly distorted tetrahedral environments with  $\text{N}-\text{Ag}-\text{N}$  angles ranging from  $100.19(2)$  to  $121.26(9)^\circ$ .  $\text{Ag}-\text{N}$  bond lengths display the result of this change in coordination number with a corresponding lengthening to  $2.324(3)$  Å for the  $\text{Ag}-\text{N}_{\text{pyridine}}$  distances and  $2.321(3)$  Å for the  $\text{Ag}-\text{N}_{\text{amine}}$  distances.

Compound **4** is the consequence of a second equivalent of 4-amp being added to solutions that produced the one-dimensional polymer **1**. The resulting linear polymer seen in Figure 4 displays a 2:1 ratio of ligand to metal, as well as the small 4-amp box building block reminiscent of the previous structure, **3**. The polymer in this case, however, is much bulkier due to the formation of the “box-in-box” network shown. The unique portion of this structure is shown in Figure 5. The  $\text{C}9-\text{C}8-\text{C}7-\text{N}3$  torsion angle here is  $66.0(2)^\circ$ , corresponding to a rotation of the methylene-amine

bond away from perpendicular to the pyridyl. This assists in causing a lengthening of the cross-box  $\text{Ag}-\text{Ag}$  distance to  $6.9946(4)$  Å as well as a concomitant separation of the adjacent pyridyl  $\pi$ -systems to around 3.45 Å. Opposing silver-occupied corners of two separate small boxes are subsequently bridged by another 4-amp ligand to construct the box-in-box motif seen in the figure. The open corners of this larger box are occupied by amine nitrogens which have a much greater diagonal distance at  $13.577(3)$  Å. The conformation of this second ligand is different from that of the first as seen by the change in the analogous torsion angle,  $\text{C}3-\text{C}2-\text{C}1-\text{N}1$ , to a more acute  $39.8(2)^\circ$ . A difference in bond lengths is also seen between silver and those ligands that are either involved in the construction of the small box or those that bridge the smaller boxes together, with the intrabox bonds apparently being a bit stronger. In-box silver-pyridyl and silver-amine distances are  $2.391(1)$  and  $2.276(1)$  Å, respectively, whereas the bridging 4-amp has corresponding distances a bit longer at  $2.431(1)$  and  $2.346(1)$  Å. The tetrahedral environment of the metal center here is also slightly more distorted than in the previous structure with  $\text{N}-\text{Ag}-\text{N}$  angles ranging from  $92.07(4)$  to  $119.90(5)^\circ$ . The noncoordinating  $\text{OTf}^-$  anions sit within the cavities formed by the larger box and are held in place by H-bonding to the amine nitrogens.

Keeping with the box-in-box motif is compound **5**, which is again based upon the symmetric biligand, bimetallic box of the previous two structures. Polymeric growth in this case, however, extends to form a two-dimensional box-in-box network as shown in Figure 6. The small box is once more seen to occupy opposite corners of a larger box constructed of linkages formed by an outward-facing 4-amp ligand. In the current case the larger box is of much greater size due to the incorporation of two bridging ligands, each being used to form the remaining two corners of the box. These corners both terminate with a silver(I) cation; the two metals are separated by a  $20.0112(6)$  Å span. The smaller box sees its shortest  $\text{Ag}-\text{Ag}$  separation discussed herein at  $6.5094(3)$  Å. This is associated with a rotation of the  $-\text{CH}_2-\text{NH}_2-$  bond closer to perpendicular to the pyridyl plane, with the  $\text{C}6-\text{C}2-\text{C}1-\text{N}2$  torsion angle being  $73.0(3)^\circ$ . Interestingly, the adjacent pyridyl rings in this case are along the same separation as those in the structure of **4**, with an approximate division of 3.45 Å. The unique portion of **5** is displayed in Figure 7 and shows the similarities between the conformations of the  $\text{N}1$  (small box) ligand and the  $\text{N}3$  (bridging)

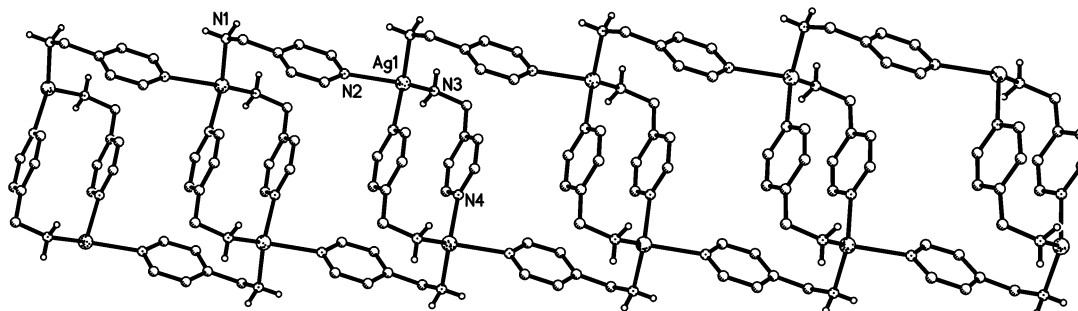


**Figure 4.** View of the cationic “box-in-box” structure of **4**. Anions and all hydrogen atoms except for those on the amines have been removed for clarity.

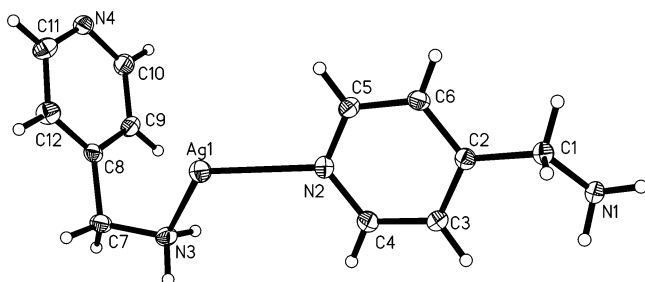


**Figure 5.** Thermal ellipsoid plot of the unique cationic portion of **4**. Ellipsoids are drawn at the 50% probability level. The anion is not shown for clarity.

ligand with only a rotation of the methylene–amine vector differentiating the two; the C9–C8–C7–N4 torsion angle is  $92.4(3)^\circ$ . Silver–pyridyl and silver–amine bond distances of the small box are again seen to be shorter at 2.280(2) and 2.327(2) Å than the open ligand with analogous lengths of 2.380(2) and 2.347(2) Å, respectively. Tetrahedral N–Ag–N angles range from  $99.86(7)$  to  $126.6(7)^\circ$ .

Compound **6** was synthesized in order to study the effects of adding a strongly chelating ligand on the polymerization of the 4-amp complexes. However, repeated attempts at crystallization consistently produced poor quality crystals from which little could be established. As a result, 5,5'-dimethyl-2,2'-bipyridine was used as a model which was expected to have similar coordination properties, and we were able to obtain satisfactory diffraction quality crystals of **6a**.

When 5,5'-dimethyl-2,2'-bipyridine is added to solutions of 4-amp with silver(I)  $\text{BF}_4^-$ , ligand bridged polymerization into the structures seen previously<sup>50</sup> and in **5** is impeded. Instead, the bipy-truncated structure shown in Figure 8 is formed. As expected, the chelating bipyridine preferentially binds the silver(I) cation, displacing the monodentate amine or pyridine of the 4-amp ligand from its coordination sphere to form the bridged bimetallic monomer of **6a**. It is seen that as long as there is sufficient 5,5'-dimethyl-2,2'-bipy present to make a 1:1 ratio of bipy to metal the stoichiometry of 4-amp in the reaction is irrelevant. A bipyridyl complex

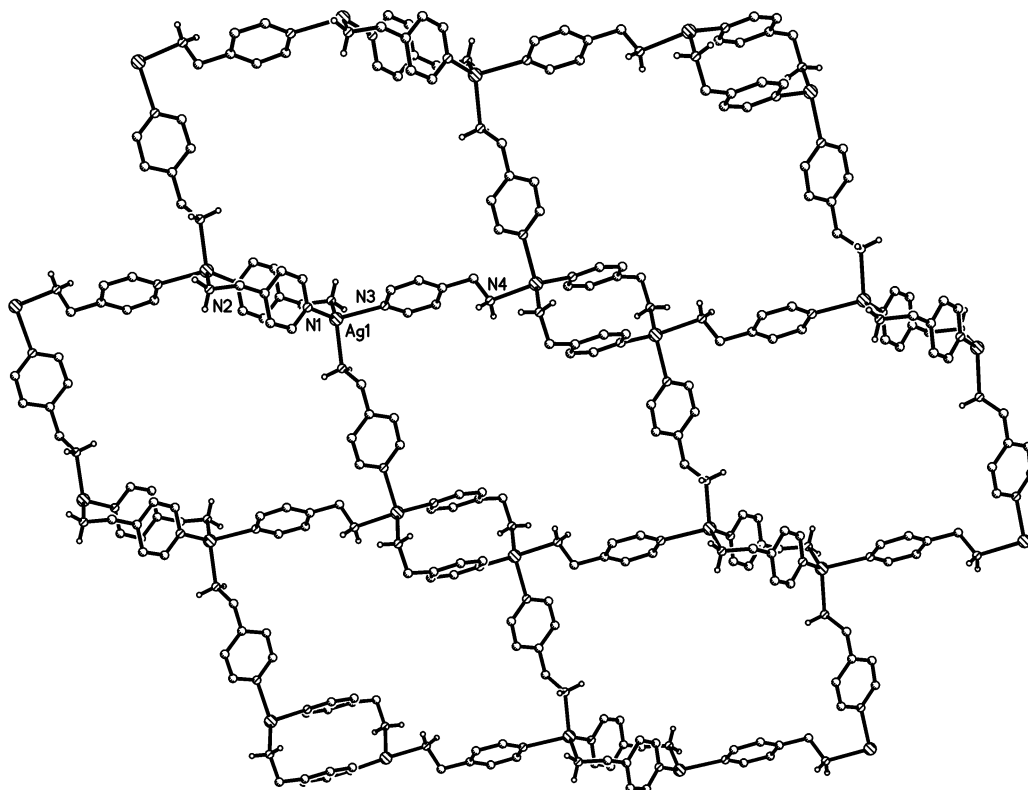


**Figure 6.** Extended view of the cationic “box-in-box” network of **5**. Anions and all hydrogen atoms except for those on the amines have been removed for clarity.

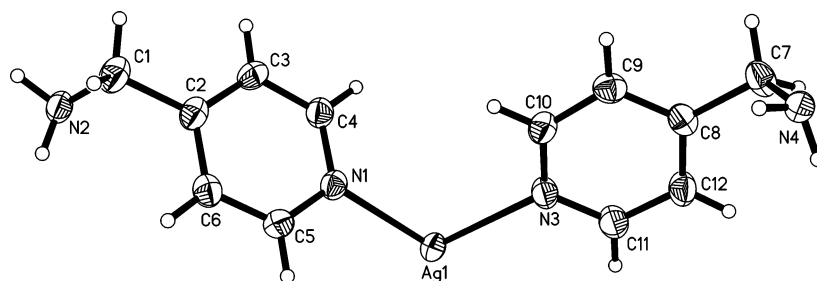


**Figure 7.** Molecular structure of the unique portion of the cationic polymer of **5**. Ellipsoids are drawn at the 50% probability level. The anion is not shown for clarity.



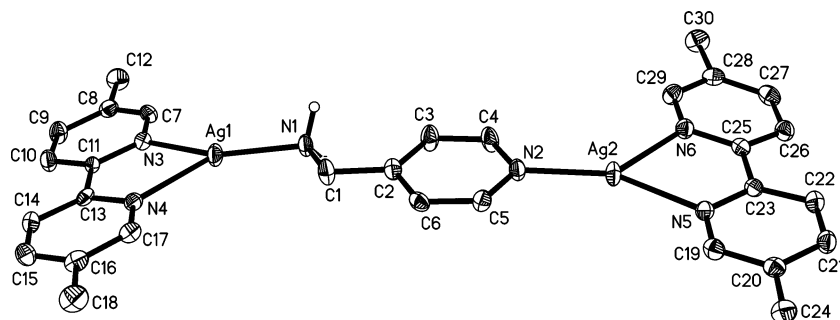


**Figure 8.** Molecular structure of the bimetallic monomer of **6a**. Ellipsoids are drawn at the 50% probability level. All hydrogen atoms except for those on the amine have been removed for clarity. Solvent molecules of crystallization and the anions have been removed for clarity.

with a higher ratio of 4-amp to silver than 0.5:1 has been so far elusive, even in the presence of a large excess (~4-fold) of the aminomethylpyridine. There are two unique silver(I) environments present in **6** due to the asymmetric nature of the 4-amp bridge. The amine-bound silver is in a slightly distorted trigonal planar environment with variance from the ideal  $120^\circ$  angles, a result of the small bite angle of the bidentate bipyridyl. Angles around Ag1 range from  $72.8(1)$  to  $150.2(1)^\circ$ . However, the metal cation is only slightly removed from its  $N_3$  plane by  $0.033(2)$  Å. Ag2 sees similar deviations from the ideal with N–Ag–N angles of  $73.1(1)$ – $153.94(1)^\circ$  and an  $N_3$  plane displacement of  $0.042(2)$  Å. The three aromatic rings bound to Ag2 give the metal a planar surrounding allowing easier access to it than Ag1, which has the amine protons protruding above and below the plane. As a result, the coordination sphere of Ag2 also contains a symmetry equivalent metal situated both directly above and below the plane of the molecule, giving the pyridyl-bound silver a metal-capped trigonal bipyramidal environment. The Ag–Ag interactions are typical lengths<sup>53–56</sup> at  $3.348(1)$  Å and appear to be supported by the  $\pi$ -stacking of pyridyl and bipyridyl rings bound to the metals. A particularly unique and interesting feature of this structure that is seen when the molecule is expanded along the direction of the metal–metal interactions, as in Figure 9, is that it is actually a linear polymer connected by an infinite metal–metal backbone. This backbone shows only a slight bend at each metal center with a Ag–Ag–Ag angle of  $174.85(2)^\circ$ . Relevant literature and CCDC searches reveal this type of polymerization to be previously unseen, with the only other infinite silver-linked polymers known being held together by bridging ligands.<sup>57,58</sup> Perpetuation of the polymer sees the molecular axis of each monomer shifted nearly perpendicular to those adjacent to it to give the overall polymer a saw tooth appearance. The C3–C2–C1–N1 torsion angle of the bridging 4-amp ligand has a value similar

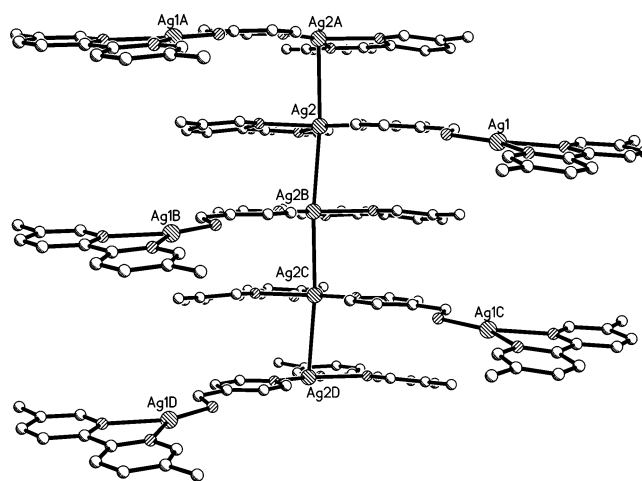


**Figure 9.** Ball-and-stick diagram showing the polymeric nature of **6a**. Anions, solvent molecules of crystallization, and hydrogen atoms have been removed for clarity.

to that seen in the 1:1 structures at  $7.4(6)^\circ$ . Ag–pyridyl and Ag–amine distances are also reminiscent of **1** and **2** at  $2.138(3)$  and  $2.161(3)$  Å, respectively. Ag– $N_{\text{bipy}}$  distances are slightly longer at  $2.256(3)$  and  $2.335(3)$  Å to Ag1 and  $2.240(3)$  and  $2.339(3)$  Å to Ag2, which are typical for Ag– $N_{\text{bipy}}$  bonds.<sup>31–33</sup> The  $\text{BF}_4^-$  anions here sit in the space formed directly behind the amines in the polymer and are held in place by weak H-bonds.

## Conclusions

Herein we have shown how the structures of supramolecular compounds of the ligand 4-aminomethylpyridine with salts of the silver(I) cation are able to be varied not only by the traditional methods such as anion control but also by changes in ratio of ligand to metal. The amine group present on the ligand allowing for H-bonding of the resultant complexes as well as an inclination for the 4-amp ligand to participate in  $\pi$ -stacking interactions also contributes to the overall conformations of the structures presented which display several different one- and two-dimensional motifs. Studies of the amp ligands are being continued with mixed ligand systems as well as the asymmetric methylpyridine– and bis(methylpyridine)–aminomethylpyridines.

**Acknowledgment.** This research was supported by funds provided by a grant from the Robert A. Welch Foundation (AA-1508). The Bruker X8 APEX diffractometer was

(53) Fernández, E. J.; López-de-Luzuriaga, J. M.; Monge, M.; Rodríguez, M. A.; Olga Crespo, M.; Gimeno, C.; Laguna, A.; Jones, P. G. *Inorg. Chem.* **1998**, *37*, 6002–6006.

(54) Hermann, H. L.; Boche, G.; Schwerdtfeger, P. *Chem. Eur. J.* **2001**, *7*, 5333–5342.

(55) Pyykko, P.; Runeberg, N.; Mendizabal, F. *Chem. Eur. J.* **1997**, *3*, 1458–1465.

(56) Pyykko, P.; Runeberg, N.; Mendizabal, F. *Chem. Eur. J.* **1997**, *3*, 1451–1457.

(57) Hannon, M. J.; Painting, C. L.; Plummer, E. A.; Childs, L. J.; Alcock, N. W. *Chem. Eur. J.* **2002**, *8*, 2225–2238.

(58) Hou, L.; Li, D. *Inorg. Chem. Commun.* **2005**, *8*, 128–130.

purchased with funds received from the National Science Foundation Major Research Instrumentation Program Grant CHE-0321214.

**Supporting Information Available:** Extra figures and low-temperature luminescence spectra as well as final atomic coordi-

nates, anisotropic thermal displacement parameters, and complete bond lengths and angles in CIF format are available for complexes **1–6a**. This material is available free of charge via the Internet at <http://pubs.acs.org>.

IC051659E